PAPER • OPEN ACCESS

Study on the characteristics of initial shock waves generated by cylindrical charge for underwater explosion

View the article online for updates and enhancements.

Study on the characteristics of initial shock waves generated by cylindrical charge for underwater explosion

T Ma[1], J X Wang[1], L T Liu[1], H Li[2], Y C Gu[1] and Y F Zhang[1]

1 National Key Laboratory of Transient Physics, Nanjing University of Science and Technology, Nanjing 210094, Jiangsu, China
2 Naval Armament Department, 100841, Beijing, China

Email: wjx@njust.edu.cn

Abstract. In order to provide a theoretical basis for studying the shock wave propagation and evolution generated by cylindrical charge of near-field underwater explosion, the characteristics of initial shock waves generated by cylindrical charge are studied. First, a new theoretical model for initial shock waves is proposed by the polar curve method. Based on the theoretical model and the simulated results, the influences of incident angle, length-to-diameter ratio and type of charge on the initial shock waves are analysed. Then the experiments of underwater explosion load tests are carried out to verify the theoretical and simulation results. Finally some instructive conclusions are drawn: i) The two-dimensional theoretical model can calculate the initial underwater shock wave pressure and its direction of cylindrical charge through detonation velocity, detonation pressure, explosive density and incident angle, which is provides a theoretical basic for studying the shock wave propagation and evolution studies. By comparing the theoretical results with the numerical results verified by experiments, the maximum error is not more than 9.93%. ii) Increasing the incident angle α_0 will reduce the initial shock wave pressure of cylindrical charge and make its direction deflect towards the material interface. When the incident angle α_0 is in the range of 0 - 10 °, increasing the incident angle makes the initial shock wave pressure decrease rapidly as a power function. With the increasing of the incident angle, the attenuation rate of the initial shock wave firstly decreases and then increases when the incident angle α_0 is in the range of 10 - 72 °. This phenomenon explains the reason that the axial and radial initial shock wave pressures are much higher than those in other directions after the central initiation of cylindrical charge. iii) According to the geometric relationship, the length-to-diameter ratio of the charge will limit the range of the incident angle. The length-to-diameter ratio will affect the initial shock wave pressure at the same initiation time. The pressure decreases with the increase of the length-to-diameter ratio when the initial shock wave is formed on the cylindrical surface of the charge.

1. Introduction

Underwater explosion is a basic subject on the design of underwater weapons and protective structures [1-4]. Compared with the load in air, the load formed by underwater explosion not only has high-frequency shock wave load, but also contains the unique low-frequency bubble load caused by explosion bubble expansion and contraction. Due to the different formation mechanism and damage effects of the shock waves and bubble loads, they are often studied separately when discussing the load characteristics [5-7]. Among them, there are many factors affect the characteristics of shock wave, such as the blast distance [8], type of explosive, charge shape and initiation model [9], etc. As we all know, shock wave is formed by underwater detonation of explosives. At the end of the detonation

phase, the detonation wave enters the water medium and the initial shock wave is formed. When the shape of explosive is spherical, the shock wave field formed by its explosion is also spherical [10]. At this time, the one-dimensional hypothesis is applicable to the formation process of the initial shock wave [11]. Therefore, the initial shock wave pressure is an important index to measure the underwater explosion power of explosives. And the research on the characteristics of the initial shock wave can provide a basis for the subsequent analysis of the shock wave propagation and evolution in the water [12]. However, when the explosive is cylindrical, the shock wave field formed by its explosion is ellipsoid. At this time, the pressure of the initial shock wave is changes with the direction angle, and the one-dimensional hypothesis is no longer applicable to the formation process of the initial shock wave. As one of the commonly used charge structures, there are few studies on the initial shock wave pressure characteristics of cylindrical charge. It may be because that the range of the sensor limits the underwater explosion load test, and it is difficult to directly obtain the accurate initial shock wave pressure [13]. Therefore, in order to more comprehensively describe the underwater explosion power of cylindrical explosives, it is meaningful to establish a two-dimensional axisymmetric theoretical model for the initial shock wave. And it can provide a theoretical basis for the subsequent analysis of the shock wave propagation and evolution.

In this paper, Firstly, based on two-dimensional plane hypothesis and ideal detonation hypothesis, the axisymmetric initiation model of cylindrical charge underwater explosion is established. The propagation process of detonation wave in explosive and the transmission and reflection process of detonation wave at the interface between explosive and water are analysed. The pressure and direction of initial shock wave at the interface between explosive and water are solved by polar curve method. Then, the underwater explosion load test and numerical simulation of cylindrical charge are carried out. Finally, according to the theoretical model and the simulated results, the influences of incident angle, length-to-diameter ratio and type of charge on the initial shock waves are analysed.

2. Theory analysis of initial shock wave in underwater explosion generated by cylindrical charge

In underwater explosion, the shock wave goes through the detonation process, the propagation process of detonation wave in the explosive, the transmission and reflection process of the interface between detonation wave and water, and the propagation process in water, and finally reaches any position in space. The detonation wave is transmitted and reflected on the interface between explosive and water, and finally the initial shock wave is formed. Therefore, when calculating the initial shock wave pressure, it is necessary to analyse the detonation phenomenon of explosive detonation and the transmission and reflection process of wave on the interface between explosive and water.

2.1 Analysis of detonation wave propagation process in explosive

It is assumed that the detonation process of explosives is an ideal detonation and the detonation wave propagation process is an isentropic process. When the C-J surface formed by detonation wave reaches the boundary of cylindrical explosive, the relevant parameters on the continuous interface can be expressed as Eqn. (1) - (4) [14].
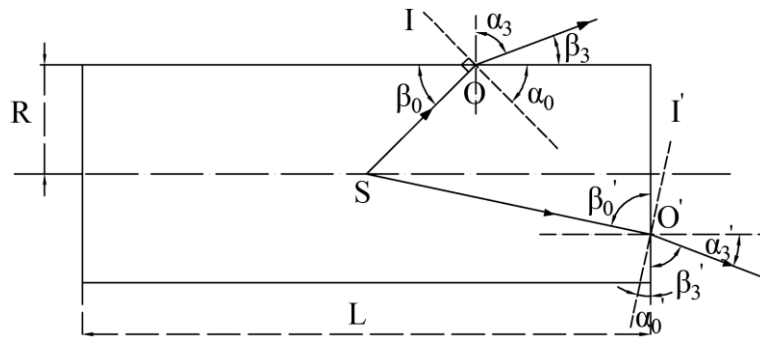
$$p_j = \frac{1}{k+1}\rho_0 \cdot D^2 \tag{1}$$

$$\rho_j = \frac{k}{k+1}\rho_0 \tag{2}$$

$$u_j = \frac{1}{k+1}D \tag{3}$$

$$C_j = \frac{k}{k+1}D \tag{4}$$

where p_j、ρ_j、u_j、c_j are the C-J pressure, density, particle velocity and sound velocity of detonation wave, respectively. D is the detonation velocity. ρ_0 is the initial density of the charge. k is the isentropic index.

Figure 1. Calculation model of initial shock wave pressure of cylindrical explosive

When the explosive is detonated, the detonation wave propagates inside the explosive. The detonation wave reaching the interface between explosive and water is shown in Figure 1. Where, point S is the initiation point. R is the radius of cylindrical explosive. L is the height of cylindrical explosive. The angle between the propagation direction of detonation wave and the cylindrical surface of explosive is β_0. The angle between the incident wave front and the cylindrical surface is α_0. The direction angle of the transmitted wave is β_3. Similarly, when the detonation wave reaches the end of cylindrical explosive, the angle between the propagation direction and the end face is β_0', the angle between the incident wave front and the end face is α_0', the direction angle of the transmitted wave is β_3'.

According to the geometric relationship on the interface of the cylindrical charge, the relevant angle between the incident wave front and the explosive boundary can be expressed by Eqn. (5) and Eqn. (6).

$$\sin\beta_0 = \sin(\pi - \alpha_0) = \frac{R}{D \cdot t} \tag{5}$$

$$\sin\beta_0' = \sin(\pi - \alpha_0') = \frac{L/2}{D \cdot t} \tag{6}$$

where t is the propagation time of detonation wave inside the charge.

2.2 Analysis of transmission and reflection process of detonation wave

When the detonation wave reaches the interface between the explosive and water, the transmission and reflection process of detonation wave are shown in Figure 2. Where, the **OF** is the interface between explosive and water medium. The detonation shock wave front is **OI**. The reflected shock wave front is **OR**, and the transmitted shock wave front is **OT**. The undisturbed interface **OF** will turn into **OF'** after the action of detonation wave. Since the wave impedance of explosive is greater than that of water, the reflected wave is a sparse wave. If the inhomogeneity of the reflected rarefaction wave is neglected, the interface in figure 2 and wave front of water and explosive divide the water field into five regions. Zone (0) is the undisturbed region in the explosive. Zone (0') is the undisturbed region in water. Zone (1) is the post wave region of the incident wave **OI** and also the wavefront region of the reflected wave **OR**. Zone (2) is the post rarefaction wave region in the explosive. Zone (3) is the post transmission wave region in water. The disturbed interface **OF'** distinguishes the zone (2) and zone (3).
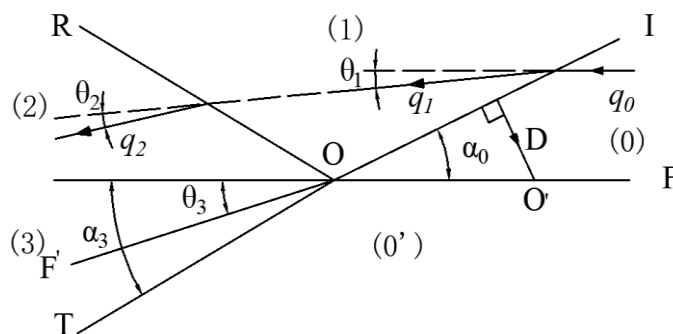
Figure 2. Diagram of incident wave front reaching cylindrical explosive interface

The flow velocity in the laboratory coordinate and moving coordinate system is expressed as $\boldsymbol{u}$ and $\boldsymbol{q}$, respectively. The point O in the laboratory coordinate system is opposite to that of the vector $\boldsymbol{q_0}$, then from the vector and geometric relationship in Figure 2, we can obtain Eqn. (7-10).

$$\boldsymbol{q_i} = \boldsymbol{u_i} + \boldsymbol{q_0} \tag{7}$$

$$q_0 = \frac{D}{\sin \alpha_0} \tag{8}$$

$$q_1 = (q_0 - u_1 \sin \alpha_0)^2 + u_1^2 \cos^2 \alpha_0 \tag{9}$$

$$\tan \theta_1 = \frac{u_1 \cos \alpha_0}{q_0 - u_1 \sin \alpha_0} \tag{10}$$

where $\boldsymbol{\theta_1}$ is the angle between vector $\boldsymbol{q_0}$ and $\boldsymbol{q_1}$.

2.2.1 Reflection process analysis of detonation wave

It is assumed that the detonation wave is not affected by the reflected rarefaction wave. Therefore, the incident wave velocity in zone (1) in Figure 2 is equal to the detonation velocity D. The velocity, pressure and density of the fluid pellet in zone (1) are $\boldsymbol{u_1}$, $\boldsymbol{p_1}$ and $\boldsymbol{\rho_1}$, respectively. When rotating counterclockwise from $\boldsymbol{q_0}$ to $\boldsymbol{q_1}$, the angle is positive. Therefore, according to the pole curve relationship of shock wave and the Hugoniut relationship, we can obtain Eqn. (11-12).

$$\frac{d\theta_2}{dp_2} = -\frac{\sqrt{M^2 - 1}}{\rho_2 q_2^2} \tag{11}$$

$$\frac{q_2^2}{2} = \frac{q_1^2}{2} - \int_{p_1}^{p_2} \frac{dp}{\rho} \tag{12}$$

It is assumed that the explosive is a polytropic gas and the reflection process is isentropic. Therefore, the relationship between the pressure, density and sound velocity on the reflected wave front can be expressed as Eqn. (13, 14) [14].

$$\frac{\rho_2}{\rho_1} = \frac{(k_1 + 1)p_2 + (k_1 - 1)p_1}{(k_1 + 1)p_1 + (k_1 - 1)p_2} \tag{13}$$

$$c_2^2 = k_1 \frac{p_2}{\rho_2} \tag{14}$$

where the density and pressure of the charge in zone (2) are expressed as $\boldsymbol{\rho_2}$ and $\boldsymbol{P_2}$, respectively. $\boldsymbol{\theta_2}$ is the angle between vector $\boldsymbol{q_1}$ and $\boldsymbol{q_2}$. The isentropic index $\boldsymbol{k_1}$ of polytropic gas is 1.4.

2.2.2 Transmission process analysis of detonation wave

The wave impedance of water is less than that of explosive, so the transmitted wave is compression wave. The hydrostatic pressure, density and velocity of the fluid pellet in zone (0') is $\boldsymbol{p_0}'$, $\boldsymbol{\rho_0}'$, and $\boldsymbol{u_0}'$, respectively. The velocity in the moving coordinate system is $\boldsymbol{q_0}'$, then:

$$\boldsymbol{q_0'} = \boldsymbol{q_0} + \boldsymbol{u_0'} \tag{15}$$

The polar curve of the transmitted wave in zone (3) can be expressed as Eqn. (16).

$$\begin{cases} \tan \theta_3 = \dfrac{\sqrt{\lambda \left(\dfrac{1}{\rho_0'} - \dfrac{1}{\rho_3'} \right) - \left(\dfrac{\lambda}{\rho_0' q_0'} \right)^2}}{q_0' - \dfrac{\lambda}{\rho_0' q_0'}} \\ \lambda = p_3 - p_0' \end{cases} \tag{16}$$

When water is in under compression state, the polynomial equation of state can be used to describe the relationship between pressure and density in the zone (3). Then:

$$p_3 = A_1 \mu + A_2 \mu^2 + A_3 \mu^3 + (B_0 + B_1 \mu)\rho_0' E_M \tag{17}$$

$$\rho_3^{'} = (\mu + 1)\rho_0^{'} \tag{18}$$

Where, p_3 is the transmitted wave pressure in zone (3); θ_3 is the angle between the explosive interface **OF** and **OF'**. μ is the compression ratio of water. p_0' is the density of water without disturbance.

2.2.3 Calculation process

As shown in Figure 2, the reflected wave disturbance zone (2) in explosive and the transmitted wave disturbance zone (3) in water medium are separated by the interface **OF'**. According to the interface continuity conditions and the geometric relationship in Figure 2, the relationship of the parameters in interface OF' can be expressed as Eqn. (19) - (21).

$$q_2 \, /\!/ \, q_3 \, /\!/ \, \mathbf{OF}^{'} \tag{19}$$

$$p_2 = p_3 \tag{20}$$

$$\eta = \theta_3 - (\theta_1 + \theta_2) = 0 \tag{21}$$

Since the reflection and the transmission interface meet the continuity assumption and momentum conservation conditions, the reflected wave polar curve must pass though point (θ_1, p_1), the transmitted wave polar curve must pass through point $(0, p_0')$. According to sections 1.2.1 and 1.2.2, the initial shock wave pressure is the intersection of reflection and transmission polar curves, represented by Eqn. (10), (11) and (16). And Eqn. (22) is obtained by Eqn. (10), (11) and (16).

$$\begin{cases} \arctan\left(\dfrac{\sqrt{\lambda\left(\dfrac{1}{\rho_0^{'}} - \dfrac{1}{\rho_3^{'}}\right) - \left(\dfrac{\lambda}{\rho_0^{'}q_0^{'}}\right)^2}}{q_0^{'} - \dfrac{\lambda}{\rho_0^{'}q_0^{'}}}\right) - \left(\arctan\left(\dfrac{u_1\cos\alpha_0}{q_0 - u_1\sin\alpha_0}\right) - \displaystyle\int_{\theta_1}^{\theta_2} \dfrac{\sqrt{M^2 - 1}}{\rho_2 q_2^2} dp_2\right) = \eta \\[2em] p_3 \in (p_0^{'}, p_1) \end{cases} \tag{22}$$

The direction of the initial shock wave β_3 is expressed by the angle between interface **OT** and **OF**, which can be obtained by Eqn. (23).

$$\beta_3 = \pi - \arctan\left(\frac{1}{q_0^{'}} \sqrt{\frac{p_3 - p_0^{'}}{\rho_0^{'}\left(1 - \dfrac{\rho_0^{'}}{\rho_3^{'}}\right)}}\right) \tag{23}$$

3. Experiments

This section describes the underwater explosion load test. Some test results will be used to verify the theoretical model and numerical simulation results.

Fig. 3 shows a 3D schematic of the test arrangement. The test is carried out in a 2 m $\times$ 2 m $\times$ 2.3 m water tank, with a water depth of 2 m and an observation window of 0.6 m $\times$ 0.6 m. Heavy objects are suspended at the bottom of the three free-field water pressure sensors so that the sensors and explosives are located at a depth of 1 m. The sensors are arranged circularly with directions of 0° (axial), 45°, and 90° (radial). The pressure sensor used in the test is W138A05 provided by the PCB company. The voltage of the sensor is ± 5V, which is used to measure the impact pressure, and the maximum range is 34.475 MPa. In the test, the sensors in three directions are 0.5 m away from the centre of the explosive. According to Eqn. (2), it is estimated that the peak pressure of 10 g spherical explosive TNT at 0.5 m is approximately 20.2 MPa, which is within the range of the pressure sensor and meets the test requirements [15].

$$P_m = 52.4 \times \left(\frac{\sqrt[3]{w}}{R}\right)^{1.13}, \tag{24}$$

Where, P_m is the peak pressure of the shock wave. w is the mass of explosive. R is the distance from the measuring point to the centre of mass of the explosive sphere, which is 12–240 times the radius of the explosive.

Fig. 4(a) shows the explosive used in the test. The size of the explosive is shown in Table 1. Fig. 4(b) shows the test pressure data-acquisition system. The system consists of a signal conditioner, data collector, and computer used for data processing. During the test, a signal conditioner and pressure sensor are connected to ensure the stability of the test voltage signal. Simultaneously, a data collector with 2 MHz sampling frequency is used to prevent "peak leakage" during measurement. Finally, the pressure-time history data for the three directions are obtained.

Table 1. Dimensions of cylindrical explosive for underwater explosion test

Weight w /g	Density ρ /(kg/m^3)	Diameter D /mm	Length L /mm
10	1550	20	20
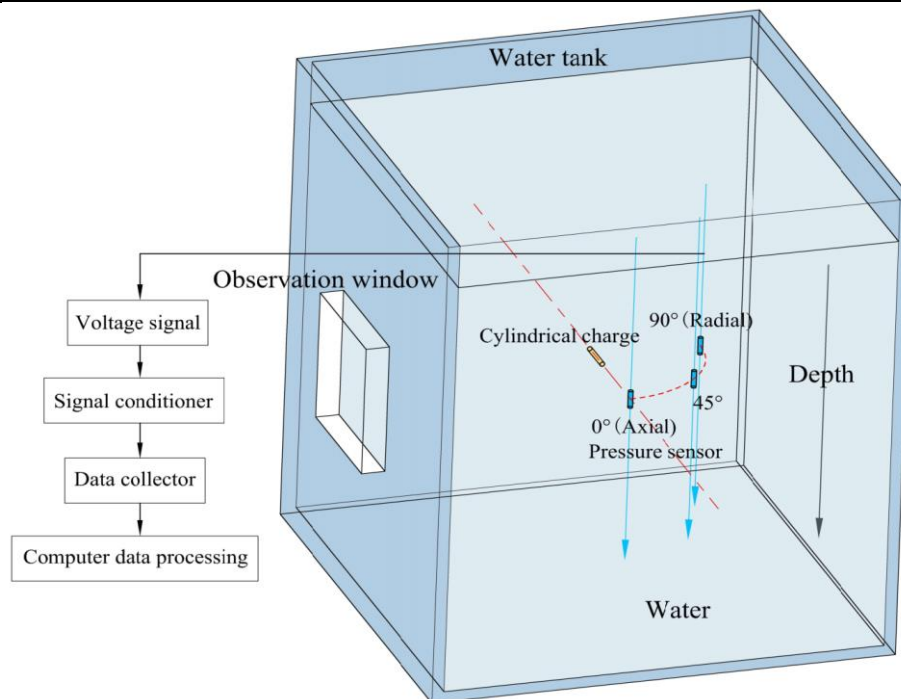
Figure 3. Diagram of underwater explosion load test

(a). Explosive   (b). Data acquisition system

Figure 4. Pictures of underwater explosion load test

4. Numerical model

Due to the range limitation in the test, only limited shock wave data can be obtained. Therefore, in order to verify the effectiveness of the theoretical calculation method, the initial shock wave pressure on the interface between explosive and water are obtained through numerical simulation.
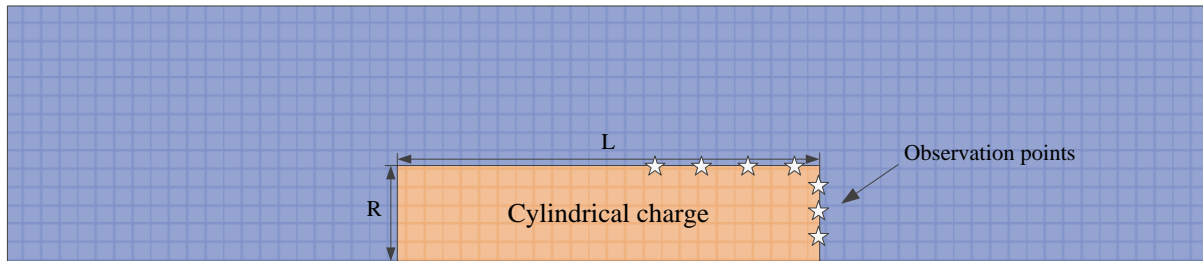
Figure 5. The enlarge view of axisymmetric FEA model nearby the cylindrical charge

4.1 FEA model and discretization

The axisymmetric FEA model is shown in Figure 5. The size of the water area is 3 m × 1.5 m. The dimensions of the explosives are listed in Table 2. 2D multi-ma Euler algorithm is used for numerical calculation. Euler grid is used for explosive and water area. The numerical domain is discretized by a transitional finite element mesh with an increasing refinement nearby the cylindrical explosive. The minimum element size is 0.1 mm × 0.1 mm nearby the charge and the maximum size is 2cm × 2 cm on the outer boundary of the water [16-18]. Non-reflecting boundary conditions are set around the water domains. The initiation point is set in the center of the cylindrical explosive at coordinates (0, 0). As shown in Figure 5, some observation points are set at the interface between explosive and water.

Table 2. Dimensions of cylindrical explosive for numerical simulation

L/D(Length-to-diameter ratio)	Weight w /g	Length L /mm	Diameter D /mm
1:1	10	20	20
2:1	10	32	16
3:1	10	42	14
5:1	10	59	11.8

4.2 Constitutive model

The equation of state for water can be described by the Mie-Gruneisen equation, defining the pressure in the compressed state as Eqn. (25) and the pressure in the expanded state as Eqn. (26):

$$P = \frac{\rho_0 C^2 \mu \left[1 + \left(1 - \frac{\gamma_0}{2}\right)\mu - \frac{a}{2}\mu^2 \right]}{\left[1 - (S_1 - 1)\mu - S_2 \frac{\mu^2}{\mu+1} - S_3 \frac{\mu^3}{(\mu+1)^2} \right]^2} + (\gamma_0 + a\mu)E \tag{25}$$

$$P = \rho_0 C^2 \mu + (\gamma_0 + a\mu)E \tag{26}$$

where the speed of shock waves in water medium is expressed as *C*. The degree of compression is expressed as μ. γ_0 is the Mie–Gruneisen coefficient. *a* is the volume correction coefficient. S_1, S_2, and S_3 are the experimental fitting coefficients. *E* is the specific internal energy per unit volume [19]. The parameters of the equations of state for water are listed in Table 3.

Table 3. Parameters of water polynomial equation of state

Material	ρ_0 /(kg/m³)	C /(m/s)	γ_0	a	S_1	S_2	S_3	E /(MPa)
Water	1025	1480	0.35	0	1.921	-0.096	0	0.2895

The JWL(Jones-Wilkins-Lee) equation of state is usually used to describe TNT explosives. It defines shock wave pressure as a function of the internal energy *E* and relative volume *V* [20]:

$$P = A\left(1 - \frac{\omega}{R_1 V}\right)e^{-R_1 V} + B\left(1 - \frac{\omega}{R_2 V}\right)e^{-R_2 V} + \frac{\omega E}{V} \tag{27}$$

where ω, **A**, **B**, R_1, and R_2 are constants that characterise the explosive characteristics, and the parameters of JWL equation of state for TNT explosives are listed in Table 4.

Table 4. Parameters of TNT JWL equation of state

Material	A/Gpa	B/Gpa	R_1	R_2	ω	E/(Gpa)
TNT	371.2	3.231	0.28	396.79	0.3	7

## 5. Theoretical model and numerical simulation verification

It is difficult to directly obtain the initial shock wave pressure through the underwater explosion load test. Therefore, the effectiveness of the numerical simulation is verified by the load test. Then the accuracy of the theoretical model is further verified by comparing the numerical and theoretical results.

Figure 6 shows the pressure-time curves obtained by simulations and experiments. The result shows that the numerical results are in good agreement with the experimental results, and the error is less than 0.9%. Therefore, the simulated results are accord well with the test results.
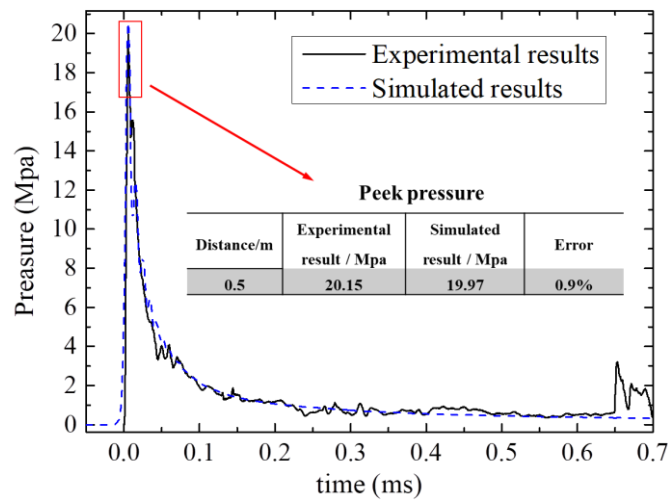
Figure 6. The simulated and experimental results of underwater explosion load test

In order to verify the effectiveness of the theoretical model, the simulated and theoretical results of the initial shock wave pressure generated by a cylindrical charge with a length diameter ratio of 3:1 are shown in Figure 7 and Table 5. With the propagation of detonation wave, the initial shock wave will be formed on the cylindrical and end boundary of the charge. The results show that the maximum error of initial pressure on the cylindrical surfaces is 9.17 %, and that of initial pressure on the end surface is 1.8 %.
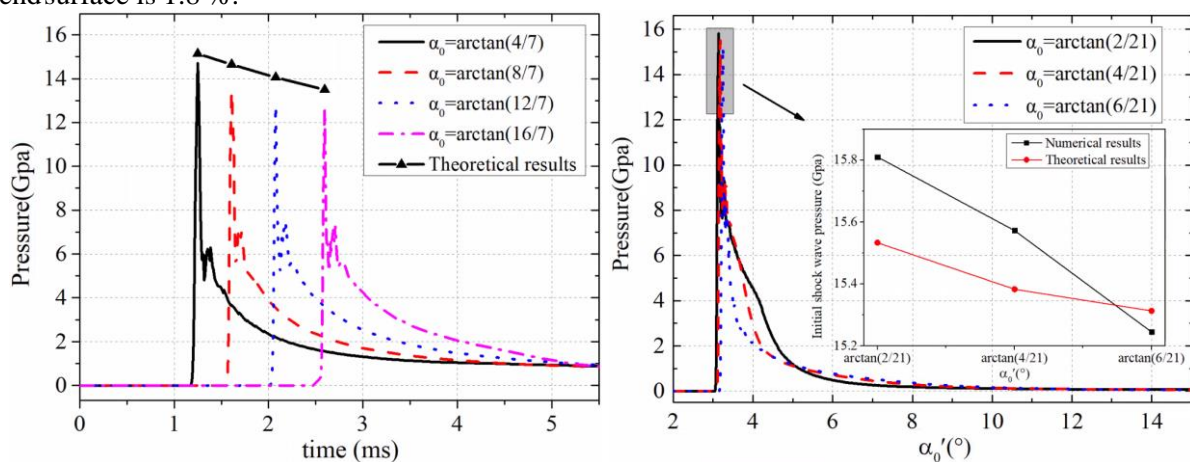
(a) cylindrical surface   (b) end surface

Figure 7. The simulated and theoretical results of initial shock wave pressure

Table 5. Comparison of theoretical models and simulated results

	Cylindrical surface				End surface		
Incident angle α_0 /°	Theoretical results /Gpa	Simulated results /Gpa	Error / %	Incident angle α_0' /°	Theoretical results /Gpa	Simulated results /Gpa	Error / %
arctan(4/7)	15.14	14.7	2.9%	arctan(2/21)	15.53	15.81	1.8%
arctan(8/7)	14.65	13.42	8.4%	arctan(4/21)	15.38	15.57	1.2%
arctan(12/7)	14.06	12.77	9.17%	arctan(6/21)	15.31	15.25	0.4%
arctan(16/7)	13.5	12.56	6.96%		/		

The theoretical model can also calculate the direction of the initial shock wave. To verify its accuracy, Figure 8 shows the pressure contour at 1.5 μs and 2 μs. The dash-dot line MI represents the material interface. The dash line TSWF represents the transmitted shock wave front. At t = 1.5 μs, the detonation wave propagates to 7.7cm in the explosive. The numerical result of the direction angle is 34 °, the theoretical result is 37.56 °. And the error between the numerical simulation and the theoretical results of the direction angle is no more than 9.47 %. At = 2 μs, the detonation wave propagates to 12cm of the position inside the explosive. The numerical result of the direction angle is 40 °, the theoretical result is 44.41 °. And the error between the numerical simulation and the theoretical results of the direction angle is no more than 9.93 %. Part of the reason for the error is that there is a systematic error in measuring the direction of the initial shock wave from the pressure contour.

Therefore, the theoretical simulation results agree well with the numerical results.

(a). t=1.5μs   (b). t=2μs
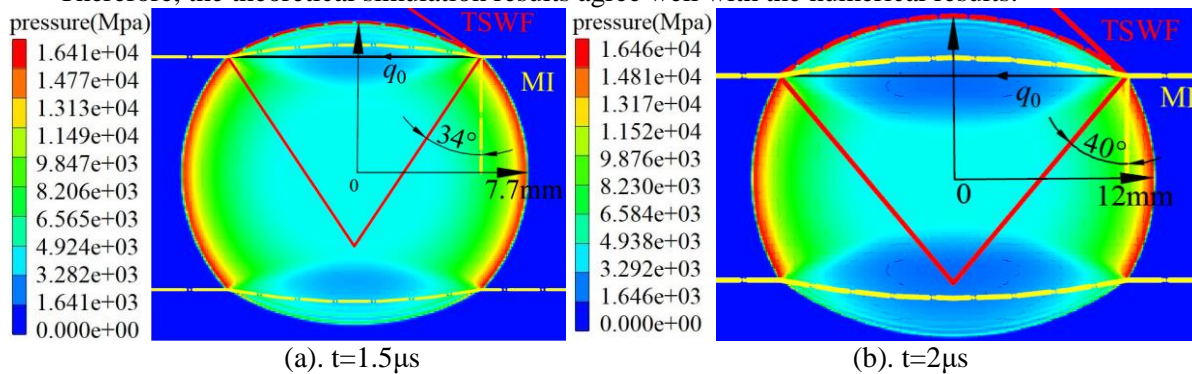
Figure 8. Initial shock wave pressure contours

6. Analysis and discussion

6.1 Influence of incident angle and type of charge on initial shock wave

The formation process of initial shock wave generated by cylindrical charge can be equivalent to the process that the detonation wave is obliquely incident on the free surface. Therefore, the incident angle α_0 has a great influence on the initial shock wave pressure and direction.


(a).   (b).
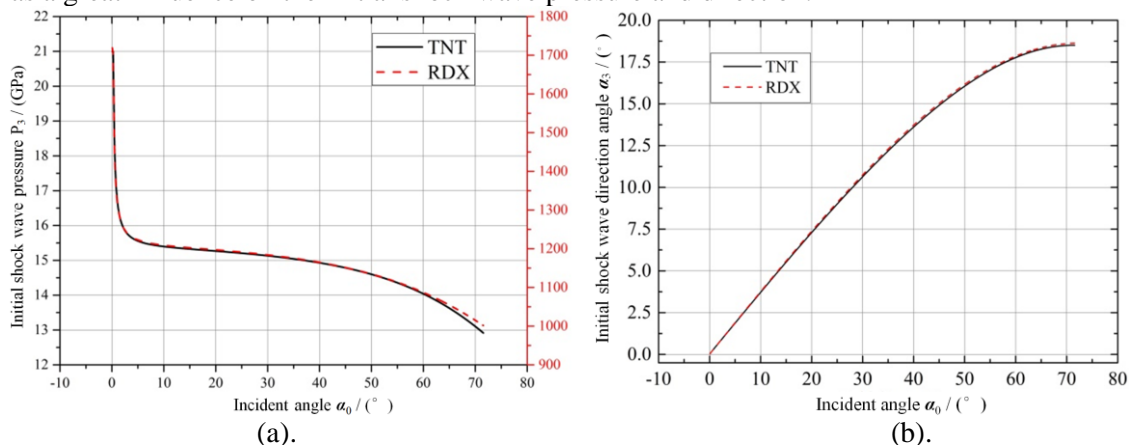
Figure 9. The α_0-P and α_0-α_3 curves are obtained by the theoretical model

As the shown in Figure 9, the α_0-p_3 and α_0-α_3 curves are obtained by the theoretical model. With the incident angle α_0 increases from $0°$ to $72°$, the initial shock wave pressure decreases gradually and the angle α_3 increases. When the incident angle α_0 is in the range of $0 - 10°$, increasing the incident angle makes the initial shock wave pressure decrease rapidly as a power function. When the incident angle α_0 is in the range of $10 - 72°$, the attenuation rate of the initial shock wave firstly decreases and then increases with the increasing of the incident angle. This phenomenon explains the reason that the axial and radial initial shock wave pressures are much higher than those in other directions after the central initiation of cylindrical charge. And with the propagation of the detonation wave, the direction of the initial shock wave will gradually deflect towards the material interface.

When the shape of the charge is spherical, the type of explosive determines the initial shock wave pressure. When the charge shape is cylindrical, the type of explosive also has a great influence on the initial shock wave pressure and its direction. It can be seen from the Figure 9, there are the similar variance tendency between the α_0-p_3 and α_0-α_3 curves generated by TNT and RDX charge. When the incident angle α_0 is the same, the initial shock wave pressure has the liner relationship between the TNT and RDX charge. Therefore, the type of explosive does not affect the relationship between the incident angle and the initial shock wave. The initial shock wave of cylindrical charge is still jointly determined by the density of charge ρ_0, detonation pressure p_j and velocity D.

6.2 Influence of the Length-to- diameter ratio on initial shock wave

According to the geometric relationship, the length-to-diameter ratio of the charge will limit the range of the incident angle. Figure 10 shows the contours of initial shock wave generated by equal mass cylindrical charge with L/D = 2:1, 3:1 and 4:1, respectively. At t = 2μs, the shock wave propagates to 14 mm of the position inside the explosive. When the length-to-diameter ratio increases from 2:1 to 5:1, the incident angle α_0 increases from $55.15°$ to $65.08°$, and the direction of the initial shock wave β_3 increases from $38 - 41°$. Comparing the data in Table 6, according to the numerical simulation calculation, the initial shock wave pressure decreased from 13.83 to 12.97 MPa. According to theoretical calculation, the initial shock wave pressure drops from 14.28 to 13.58 MPa. The numerical simulation and theoretical results show that the length-to-diameter ratio will affect the initial shock wave pressure at the same initiation time. The pressure decreases with the increase of the length-to-diameter ratio when the initial shock wave is formed on the cylindrical surface of the charge.

(a). L/D = 2:1

(b). L/D = 3:1

(c). L/D = 5:1
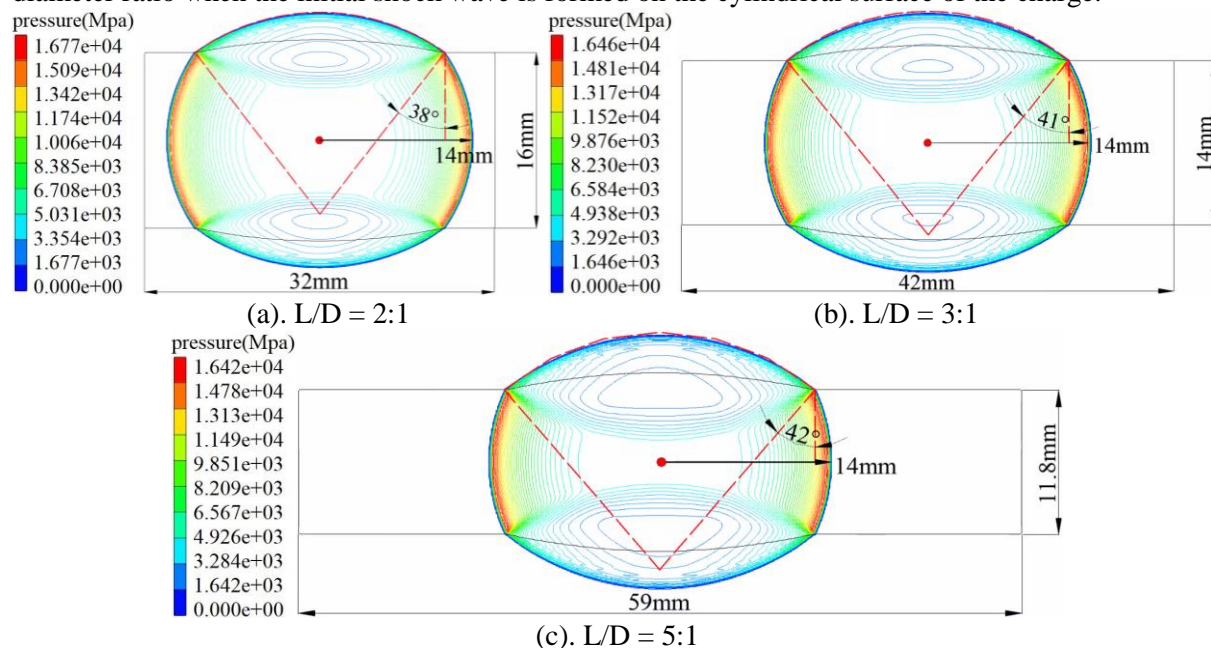
Figure 10. The contours of initial shock wave at 2 μs with different length-to- diameter ratio

Table 6. Influence of length-to-diameter on the parameters of initial shock wave at 2μs time

L/D	Incident angle/°	Direction of initial shock wave β_3/°			Initial shock wave pressure / MPa		
		Theoretical results /GPa	Simulated results /GPa	Error / %	Theoretical results /GPa	Simulated results /GPa	Error / %
2:1	55.15	41.96	38	9.4	14.28	13.83	3
3:1	60	44.42	41	7.6	13.98	13.16	5.9
5:1	65.08	46.45	42	9.5	13.58	12.97	4.5

7. Conclusions

In this manuscript, a theoretical model for initial shock waves is proposed by the polar curve method. Based on the theoretical model and the simulated results, the influences of incident angle, length-to-diameter ratio and type of charge on the initial shock waves are analyzed. Then the experiments of underwater explosion load tests are carried out to verify the theoretical and simulation results. Some instructive conclusions can be drawn from the current study:

(1) The two-dimensional theoretical model can calculate the initial underwater shock wave pressure and its direction of cylindrical charge through detonation velocity, detonation pressure, explosive density and incident angle, which is provides a theoretical basic for studying the shock wave propagation and evolution studies. By comparing the theoretical results with the numerical results verified by experiments, the maximum error is not more than 9.93%.

(2) Increasing the incident angle α_0 will reduce the initial shock wave pressure of cylindrical charge and make its direction deflect towards the material interface. When the incident angle α_0 is in the range of $0 - 10°$, increasing the incident angle makes the initial shock wave pressure decrease rapidly as a power function. With the increasing of the incident angle, the attenuation rate of the initial shock wave firstly decreases and then increases when the incident angle α_0 is in the range of $10 - 72°$.

(3) According to the geometric relationship, the length-to-diameter ratio of the charge will limit the range of the incident angle. The length-to-diameter ratio will affect the initial shock wave pressure at the same initiation time. The pressure decreases with the increase of the length-to-diameter ratio when the initial shock wave is formed on the cylindrical surface of the charge.

References

[1] Aderhold J, Davydov V Yu, Fedler F, Klausing H, Mistele D, Rotter T, Semchinova O, Stemmer J and Graul J 2001 *J. Cryst. Growth* **222** 701

[2] Ming F.R., Zhang, A.M., Xue, Y.Z., Wang, S.P. 2016 Damage Characteristics of Ship Structures Subjected to Shockwaves of Underwater Contact Explosions *Ocean Engineering* **117** 359-82

[3] Srinivas Kumar A., Umapathi Gokul K., Venkata Krushna Rao P., Jagannadham A. 2015 Blast Loading of Underwater Targets - a Study through Explosion Bulge Test Experiments *International Journal of Impact Engineering* **76** 189-95

[4] Zong Z., Zhao Y., Li H. 2013 A Numerical Study of Whole Ship Structural Damage Resulting From Close-In Underwater Explosion Shock *Marine Structures* **31** 24-43

[5] Kalavalapally R., Penmetsa R., Grandhi R. 2009 Configuration Design of a Lightweight Torpedo Subjected to an Underwater Explosion *International Journal of Impact Engineering* **36(2)** 343-51

[6] Huang C., Liu M., Wang B., Zhang Y., 2019 Underwater Explosion of Slender Explosives: Directional Effects of Shock Waves and Structure Responses *International Journal of*

        Impact Engineering **130** 266-80

[7]   Nie B., Li J. and Zhang H., 2015 On the Regimes of Underwater Explosion for a Submerged Slender Structure by Pulsating Bubble *Marine Structures* **44** 85-100

[8]   Saito T., Marumoto M., Yamashita H., Hosseini S.H.R., Nakagawa A., Hirano T. and Takayama K. 2003 Experimental and Numerical Studies of Underwater Shock Wave Attenuation *Shock Waves* **13(2)** 139-48

[9]   Cole H. 1948 *Underwater Explosions* (New Jersey)

[10]   Xiao W., Andrae M. and Gebbeken N. 2020 Influence of Charge Shape and Point of Detonation of High Explosive Cylinders Detonated On Ground Surface On Blast-Resistant Design *International Journal of Mechanical Sciences* **181** 1-11

[11]   Akio K., Masahiro F., Shigeru I. 1999 Underwater Explosion of Spherical Explosives *Journal of Materials Processing Tech* **85(1)** 64-8

[12]   Zamyshlyayev B.V. 1973 *Dynamic loads in underwater explosion* (Nav. Intell. Support. Cent.) p 86-120

[13]   Yo H.Y., Youngsik C., Joonwon L. and Kyung, J.Y. 2016 Influence of the Shape of Explosive Charge on the Blast Wave Propagation *MATEC Web of Conferences*. **54** 1-4

[14]   Hammond L. 1995 *Underwater Shock Wave Characteristics of Cylindrical Charges* (Aeronautical and Maritime Research Laboratory Ship Structures and Materials Division) p 1-10

[15]   Beijing Institute of Technology, 8 Series. 1982 *Explosion and Its Function (I)* (Beijing: National Defense Industry Press)

[16]   Barras G., Souli M., Aquelet N. and Couty N. 2012 Numerical Simulation of Underwater Explosions Using an ALE Method. The Pulsating Bubble Phenomena. *Ocean Engineering* **41** 53-66

[17]   Rajendran R. 2009 Numerical Simulation of Response of Plane Plates Subjected to Uniform Primary Shock Loading of Non-Contact Underwater Explosion *Materials & Design* **30(4)** 1000-7

[18]   Wang G., Wang Y., Lu W., Zhou W., Chen M. and Yan P. 2016 On the Determination of the Mesh Size for Numerical Simulations of Shock Wave Propagation in Near Field Underwater Explosion *Applied Ocean Research* **59** 1-9

[19]   Xu L., Wang S., Liu Y. and Zhang A. 2021 Numerical Simulation On the Whole Process of an Underwater Explosion Between a Deformable Seabed and a Free Surface *Ocean Engineering* **219(108311)** 1-6

[20]   Li X.J., Zhang C.J., Wang X.H. and Yan, H.H. 2014 Numerical Study On the Effect of Equations of State of Water On Underwater Explosions *Engineering Mechanics* **31(8)** 46-52

[21]   Shi Dang-yong, Li Yu-chun, Zhang Sheng-min 2005 *Display dynamic analysis based on ANSYS/LS-DYNA8.1* (Beijing: Tsinghua University Press)